An Experimental Investigation of the Liquefaction Resilience of Dual Row Retaining Walls using Centrifuge Modeling

Srikanth S. C. Madabhushi

Stuart K. Haigh

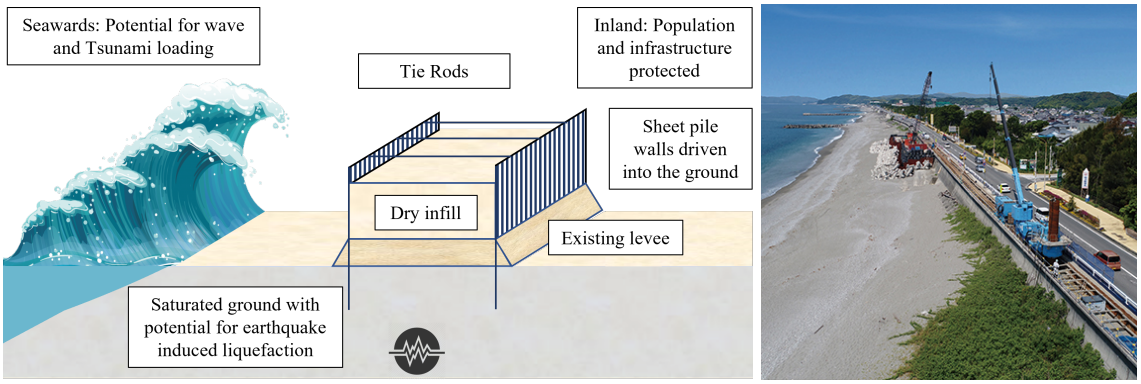
Abstract

Dual row retaining walls can be used as embankment structures and coastal defenses against wave or even Tsunami loads. However, their resilience to a preceding earthquake and liquefaction of the foundation soil is not well understood. In this paper, dynamic centrifuge modeling is used to investigate the seismic response of a dual row retaining system where the walls are founded in a loose, saturated deposit susceptible to earthquake induced liquefaction. A combination of instrumentation techniques, ranging from measurements of the wall bending and displacements to the pore pressures and horizontal earth pressures acting on the walls, are used to elucidate the mechanics of the soil-structure system. The experiments reveal that the cyclic loading does not induce a catastrophic collapse. A subtle understanding of the liquefaction phenomena, including shear induced dilation and co-seismic migration of the pore fluid towards a region of relative suction between the walls, is required to understand the observed behavior. A ratcheting mechanism for the wall deformations, consistent with the co-seismic measurements of the soil and structural response, is proposed. The findings challenge conventionally conservative design recommendations, such as the need for sheet pile walls to extend beyond a liquefiable layer to prevent liquefaction induced collapse of dual row wall systems.

1 Introduction

Dual row retaining walls are novel civil engineering systems that, through interaction between their structural and geotechnical elements, can have enhanced strength and stiffness. The design features two parallel rows of sheet pile walls with the wall heads periodically connected by tie rods. Following the installation of the two rows of sheet pile walls into an existing embankment or the ground, the space between them is typically in-filled with sand. This can achieve a large lateral capacity within a limited horizontal footprint.

In addition to forming efficient embankment structures, dual row retaining walls can be used in ports



(a) (b)

Figure 1: Conceptual schematic of dual row retaining wall used as a coastal defence, potential hazards and construction of dual row wall tsunami defence in Kochi Japan (photo from Cummins (n.d.))

or along coastlines to serve as wave or even Tsunami defense (fig. 1a). For example, following the 2011 Tōhoku Earthquake and Tsunami event, similar structures have been deployed in Kochi, Japan as illustrated in fig. 1b. In this context the resilience of the dual row retaining walls to dynamic loading when founded in saturated soils is of paramount importance. In this work the results from an experimental investigation using dynamic centrifuge modeling to investigate the overall mechanical response and resilience of the dual row retaining wall system founded in a liquefiable sand are presented.

1.1 Literature Review

Madabhushi (2018) details the combined centrifuge and finite element modeling investigation, conducted at the Schofield Centre at the University of Cambridge, of a variety of dual row retaining wall systems. Exploration of the mechanics of the systems founded in medium dense, dry sand provided a number of insights into the dual row wall behavior and fundamental findings regarding the limiting dynamic earth pressures that can be mobilized (Madabhushi and Haigh, 2020, 2021). Overall, traditionally used dynamic earth pressure coefficients ~~and their derivatives~~ with assumed geostatic vertical effective stress distributions, e.g. Okabe (1924); Mononobe and Matsuo (1929); Steedman and Zeng (1990); Choudhury and Nimbalkar (2006), were found to obfuscate the dynamic soil behavior. This was in light of the predicted dynamic vertical stress variations and observation that the static earth pressure coefficients, depending only on the soil friction angle, bounded the earth pressures mobilized during shaking.

Madabhushi and Haigh (2018a) compared the measured accelerations and displacements in experiments on similar dual row retaining wall systems, one founded in medium dense dry sand whilst the other was in a looser, liquefiable deposit. The system in dry sand showed very small permanent displacements and even stiffened with progressive cycles due to densification and the development of locked-in stresses (Madabhushi

and Haigh, 2019). However, a surprising result was that despite full liquefaction of the free field the dual row wall system in the saturated soil did not suffer a catastrophic collapse. This calls into question the typical design recommendation that the wall toes must extend to a non-liquefiable layer, e.g. Otsushi et al. (2016). In this paper a dynamic centrifuge test with a larger dual row retaining wall system featuring a variety of instrumentation techniques is used to deepen the insight into the deformation mechanics during seismic induced liquefaction of the foundation soil.

In this work the present understanding of 'general liquefied soil behavior' will be used to rationalize the experimental observations. Firstly, following the pioneering studies by Casagrande (1936); Castro (1969); Castro and Poulos (1977) and framework by Roscoe et al. (1958), the demarcation between dense (dilative) and loose (contractive) behaviors depending on the voids ratio and confining pressure is used. The 'phase transformation points' or 'characteristic state lines', as observed in both undrained cyclic triaxial testing and cyclic torsional tests (Ishihara, 1985; Luong and Sidaner, 1981), is considered an inherent transitional behavior of saturated soils and will be used to generalize the expected stress-strain behavior. This includes butterfly loops in the stress space and a banana shaped stress-strain response, i.e. implying that continued cycling at low effective stresses can result in a cyclic regain of strength and stiffness (e.g. Elgamal et al. (1998)).

More subtly, the differences between the liquefaction phenomena as observed in 'table-top' or element tests and in larger initial boundary value problems in the field or centrifuge tests must also be acknowledged (Madabhushi and Haigh, 2012; Lakeland et al., 2014). For example, recognizing the importance of co-seismic pore fluid redistribution across a large soil body may require liquefaction to be interpreted as a partially drained rather than strictly undrained ~~phenomena~~. The potential for the liquefied soil's compressibility and permeability to dramatically change may also be relevant for the co-seismic pore pressure redistribution in addition to the subsequent re-consolidation (Haigh et al., 2012).

The potential for liquefaction to cause damage and induce large displacements of coastal retaining and quay walls in the field has been widely documented following past earthquakes, ~~i.e.~~ Inatomi et al. (1997); Chen and Hwang (2000); Sumer et al. (2002). Similar observations have been replicated by dynamic centrifuge tests and numerical analyses, for example Zeng and Steedman (1993) and Madabhushi and Zeng (2007), which also highlight the potential for increased dynamic and residual bending moments in a single cantilever or tied retaining wall. On the other hand, for an excavation with a prop between two retaining walls Aversa et al. (2015) observed a relaxation and reversal of the bending moments compared to the static case, though again these were accompanied by significant wall displacements. Overall, past observations from the field and research motivates an experimental investigation of dual row retaining walls founded in liquefiable soils, and in particular their ~~resiliency~~ to large permanent deformations during and following seismic loading. A

further practical consideration will be the structural demands that are placed on the walls and connecting tie rods.

2 Centrifuge Modeling

Dynamic centrifuge modeling has been used to ~~uniquely~~ observe changes to the soil strength, stiffness and transmission of shear waves during the applied loading and liquefaction for many initial boundary value problems (Arulanandan et al., 1995; Kutter et al., 2020). A key advantage of the methodology is the similitude of the stresses and strains between the reduced scale model and equivalent full scale case, allowing the SLS and ULS performance of complex civil engineering systems to be economically tested.

Figure 2 presents a simplified schematic of the centrifuge model discussed in this paper with model and prototype scale dimensions at 60 g - the target centrifugal acceleration at 1/3 the wall height. Schofield (1980) details both the 10 m Turner beam centrifuge used and scaling laws invoked during the results presentation. The sign convention that leftward dynamic displacements, velocities and accelerations are positive is adopted. Outward bending, i.e. away from the infill, will be negative and positive for the left and right wall respectively and will be expressed per m in the out of plane direction.

The centrifuge test is identified as WF849, in reference to the saturated soil (W) up to the embedded height of the relatively flexible walls (F) and total retained, embedment and center-center wall spacing values of $8, 4$ & 9 m respectively. The walls have a thickness of 0.18 m and bending stiffness of 34 MNm^2/m, and the two connecting tie rods have a back calculated total axial stiffness of 50 MN/m (Madabhushi and Haigh,

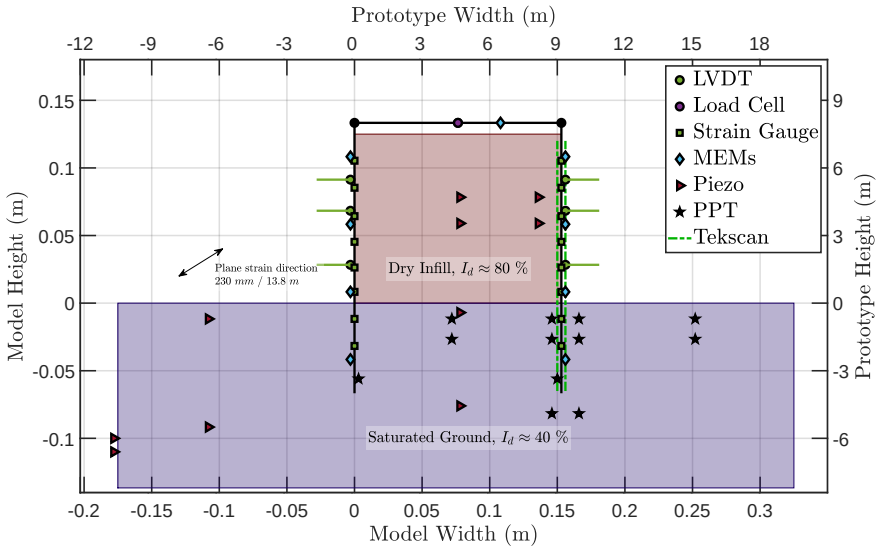


Figure 2: Cross section of centrifuge test WF849 showing model and 60 g prototype dimensions with instrumentation locations

2021). The geometry is studied to examine the liquefaction resilience of a tall wall system with a relatively small embedment which may be expected to be susceptible to toe displacements.

The model was constructed within a laminar box to minimize dynamic boundary effects (Brennan et al., 2006). S28 Hostun sand (Azeiteiro et al., 2017) was first deposited using an automatic spot pluviator (Madabhushi et al., 2006) to achieve a medium-low relative density ($I_d \approx 40$ %) to the ground surface (0 m in fig. 2). The dual row walls were placed at 1 g on a level bed of sand with pouring continued in between and around them. Above the ground level a dense infill ($I_d \approx 80$ %) was pluviated. The Cam-Sat control system (Stringer and Madabhushi, 2009) was then used to automatically saturate the centrifuge model under vacuum, following cycles of flushing the sealed model with CO_2. To satisfy consistency of the co-seismic and consolidation time scaling Hydroxypropyl Methylcellulose was used to saturated the model. This was prepared following the recommendations of Stewart et al. (1998) to achieve a dynamic viscosity 60 $\times$ greater than water at the anticipated centrifuge pit temperature.

In this paper the response of centrifuge model to a sinusoidal base excitation of ten 1 Hz cycles with an average PGA of 0.4 g per cycle is explored. This was the first large magnitude or 'destructive' motion the model was subjected to. Madabhushi and Haigh (2019) have previously described the benefits of a preceding small magnitude, 'non-destructive' motion (PGA $<$ 0.05 g that does not result in permanent structural displacements) to relieve soil arching around retaining walls that can persist during swing-up for retaining wall models constructed at 1 g.

Instrumentation used to capture the response of the centrifuge model includes full bridge strain gauges to capture the flexure of each wall, MEMs accelerometers and LVDTs to measure the wall accelerations and displacements, and Load Cells to measure the axial tie forces. Around the right wall within the saturated soil several PPTs were placed to measure the pore fluid pressures. Two additional PPTs were fixed to the left and right wall to infer the vertical settlement of the structural elements. Piezoelectric accelerometers were placed externally and in the soil during pluviation to measure the applied shaking and resulting soil acceleration. Finally, two laminated tactile pressure sensing sheets were adhered to the central portions of the wall, with the remaining areas covered with acetate to ensure consistent interfacial properties between the walls and soil. In order to obtain reliable total stress measurements from these sheets careful calibration and interpretation of the results is required, particularly for their use with granular materials (Paikowsky and Hajduk, 1997). In this work, the pressure data is processed utilizing both 1 g calibration and swing-up data as outlined in Madabhushi and Haigh (2018b) who also illustrated the consistency between the processed horizontal stresses and bending obtained from strain gauges.

3 Results

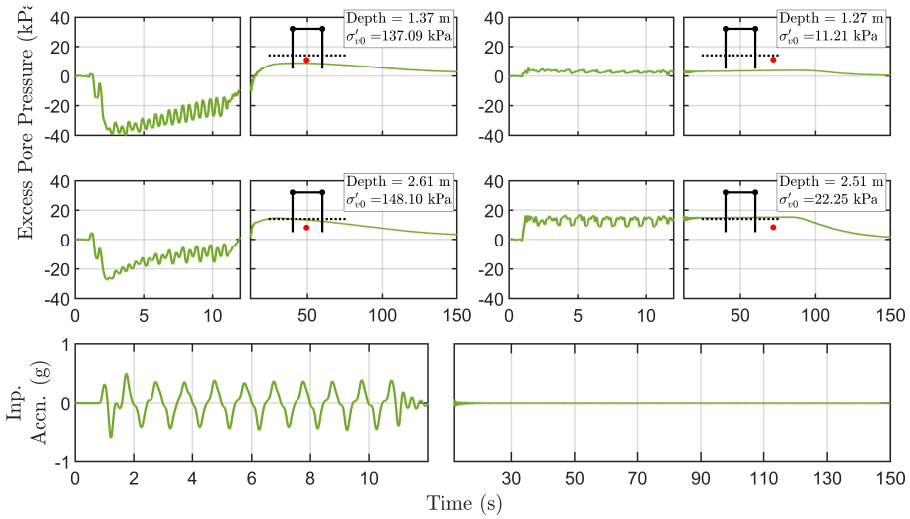
3.1 Soil Response: Pore Pressures

The generation of excess pore pressures is instrumental to understanding the dynamic experimental observations, underpinning both the bulk strength and stiffness changes to the soil. Dynamic excess pore pressures can arise from numerous physical phenomena; from the soils tendency to change volume under both normal and shear loading, due to flow driven by potential head gradients across the soil body and the fluids own ~~hydrodynamic component from its velocity.~~ Oscillations of the latter component are typically ignored based on the relatively low permeability of un-liquefied sands ($\approx 10^{-4}\ m/s$).

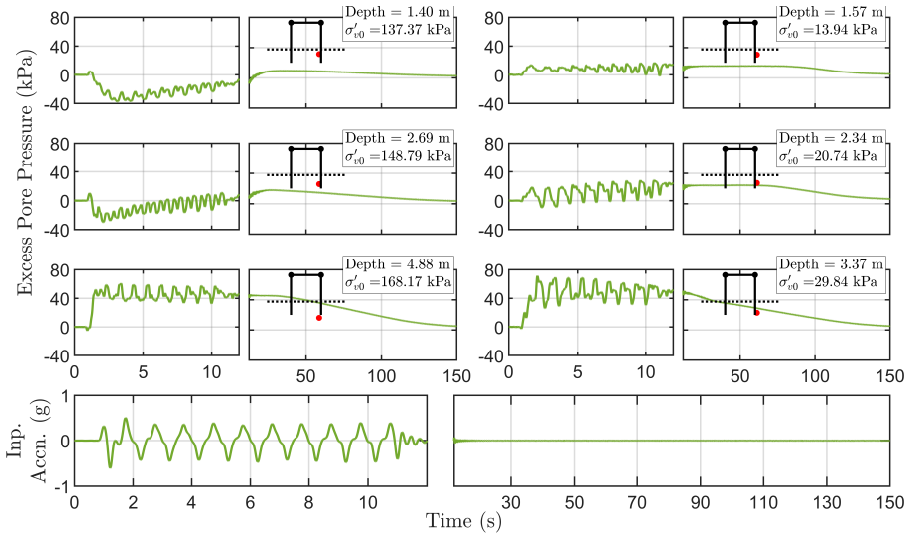
In fig. 3 the co-seismic and re-consolidation excess pore pressure time histories are presented from the infill and far field (fig. 3a) and from the transducers surrounding the right wall (fig. 3b). A schematic representation of each instrument location relative to the dual row wall system is shown, accompanied by the depth below the ground level and estimate of the initial vertical effective stress based on geostatic equilibrium. Seismic liquefaction occurrence can be identified based on the excess pore pressure ratio r_u, typically defined as the ratio of the excess pore pressure to the initial vertical effective stress or confining pressure. For the experiment described this definition is problematic for a number of reasons. Firstly, the static stress distributions, particularly near the walls, ~~is~~ difficult to theoretically predict. Secondly, it can be argued that the current effective stress should be used in place of the initial vertical effective stress. As the soil liquefies there will be a total stress re-distribution as the soil tries to equilibrate the wall system, likely via both normal and shear stresses. Further, as identified by Madabhushi and Haigh (2020, 2021) there can be significant dynamic oscillations of the vertical effective stresses around the retaining walls in addition to the expected horizontal effective stress cycling. Overall, whilst a straightforward estimate of the initial vertical effective stress is shown in fig. 3, other indications of seismic liquefaction occurrence will also be relied on.

The far field excess pore pressure time histories in fig. 3a quickly reach a plateau that, whilst lower than the theoretical initial vertical effective stress, is constant throughout the co-seismic period. Further, there is a cyclic drop or 'suction spike' observed at the shaking frequency that also indicates the shaking was sufficient to induce full liquefaction away from the walls. ~~Suction spikes at double the driving frequency are typically associated with the butterfly stress loops. The deviation may be explained by the presence of static shear stresses from the wall in the soil or the loss of upward propagation of the dynamic shear stresses, particularly in the half cycle of induced contraction.~~

The co-seismic pore pressures closer to the walls, particularly within the infill, are dramatically different. Between the walls relative suction is generally observed, with a rapid decrease from the hydrostatic values



(a) Time histories of PPTs in infill and far field, suggesting full liquefaction in the free field but relative suction between the walls



(b) Time histories of PPTs showing contrasting generation of negative and positive excess pore pressures immediately inside the right wall and below and outside the right wall respectively

Figure 3: Co-seismic and re-consolidation excess pore pressures recorded in test WF849

in the early cycles followed by a gradual increase with time. The initial decrease of the excess pore pressure can be attributed to an overall dilative tendency of the soil in this region. However, immediately below this region fig. 3b confirms the soil is trying to contract and generates positive pore pressures. Positive co-seismic pore pressures are also generated at all depths immediately outside the right wall. The observed dilative tendency of the saturated soil immediately between the walls shows that the contractile effect of the overburden stress from the dry infill has been overcome. The shaking may induce a splay displacement mode, i.e. one where the infill drives out the walls (rotating about the tie rod) and into the external soil that is softened by the positive pore pressures. However, the finite permeability and thus resistance to volumetric expansion of the saturated infill soil instead leads to negative excess pore pressures.

A reduction of the excess pore pressures below the hydrostatic value will temporarily strengthen and stiffen the saturated infill soil during the shaking, reducing the outward driving force from the soil to the walls. Nearer the surface the hydrostatic pressures are completely canceled and the pore fluid is instantaneously applying gauge suction on the soil and potentially the walls. The dynamic component of the co-seismic variation of the suctions is at double the driving frequency and relatively symmetric about an increasing mean value. An increase and decrease of suction for each half cycle of acceleration suggests the infill soil is also trying to change volume at double the driving frequency, which will be discussed when the wall displacements are examined later in this paper.

By contrast, the positive pore pressures immediately outside the wall show cyclic drops at the driving frequency and appear 'capped' in the other half. The drops may again be attributed to shear induced dilation from the wall displacement whilst the plateau the pore pressure returns to, particularly near the surface, corresponds to full liquefaction of the soil. Figure 3b shows that the suction spikes can take the external soil from fully liquefied to negligible excess pore pressures within each cycle of acceleration - implying a cyclic total loss and regaining of the soil strength and stiffness - whilst the saturated soil between the walls is not at all close to liquefying due to the large overburden stress from the dry infill and is even cyclically strengthened between the walls.

Overall there is a significant co-seismic redistribution of the pore fluid, ~~likely~~ from the lower liquefying layers upwards which partly relieves relative suction between the walls and permits volumetric change in this region. This highlights the importance of viewing liquefaction as a partially drained event across large bodies of soil. Post-seismically there is a rapid redistribution of the pore pressures that results in ~~the~~ positive excess pore pressures within the saturated infill which then dissipate as the soil re-consolidates. The coupling between the base shaking and soil stress state that lead to this transition will be explored in conjunction with the dynamic wall displacements.

3.2 Soil and Structural Response: Accelerations

The accelerations that are transmitted through the soil to the retaining wall system are coupled with the excess pore pressure generation and contribute towards the structural loading and response. In fig. 4a the vertical propagation of the soil acceleration in the free field and through the saturated and dry infill soil is shown. Following from fig. 3a, the attenuation of acceleration in the free field is as expected; the initial 'de-liquefaction shocks' (Kutter and Wilson, 1999) arising from the rapid stiffening of the liquefied but dilating soil at large strains and subsequent persistence of observable shaking at the surface; a reminder of the cyclic drops in excess pore pressure. The comparatively larger accelerations within the saturated infill are also in line with the limited positive pore pressure and relative suctions generated in those soil regions. The small accelerations in the dry infill suggests that portion of the system above the ground level remains relatively stable.

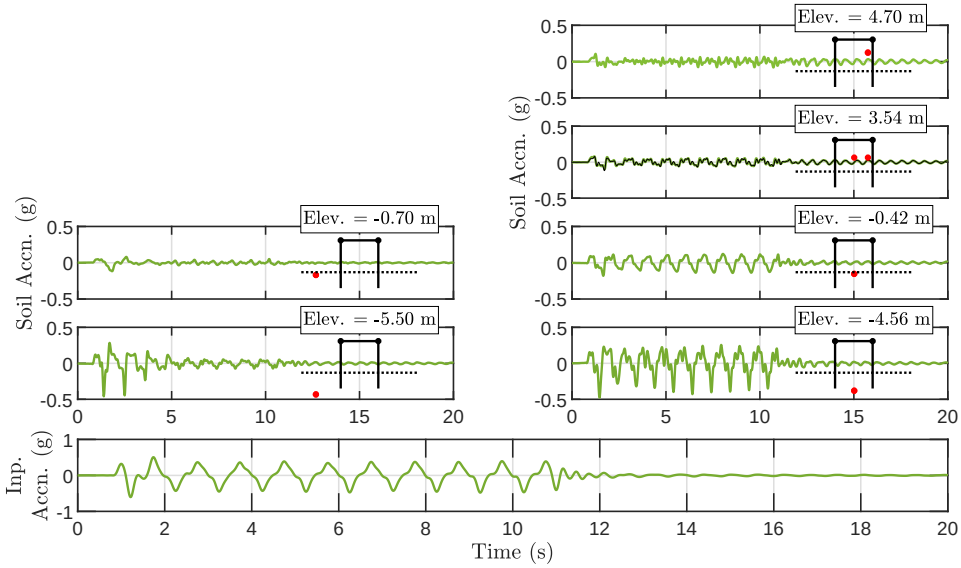
The resulting accelerations of the right and left walls are shown in fig. 4b. Overlaying the time histories shows that the left and right walls broadly accelerate in phase. However, examining the difference between the right and left wall acceleration reveals that they accelerated in the same direction by different amounts and crucially, the pattern of one wall leading another reverses every half cycle of applied base shaking. Combining fig. 3 and fig. 4 suggests that the walls, rather than displacing continuously, may experience deformations in a ratcheting fashion. This is to say that when the overall system is driven rightwards the right wall will displace relatively rightward, and similarly when the system moves left the left wall has an additional leftward displacement. The increasing discrepancy between the right and left wall acceleration down the wall height is indicative of an opening up of the wall toes and rotation about the tie rod. It is noteworthy that this is a relatively progressive failure mechanism rather than a sudden, catastrophic collapse of the dual row wall system that would be expected if a simplistic interpretation of the liquefaction phenomena as a binary loss of soil strength and stiffness is imagined.

3.3 Soil and Structural Response: Wall Displacement and Flexure, Horizontal Stresses and Tie Forces

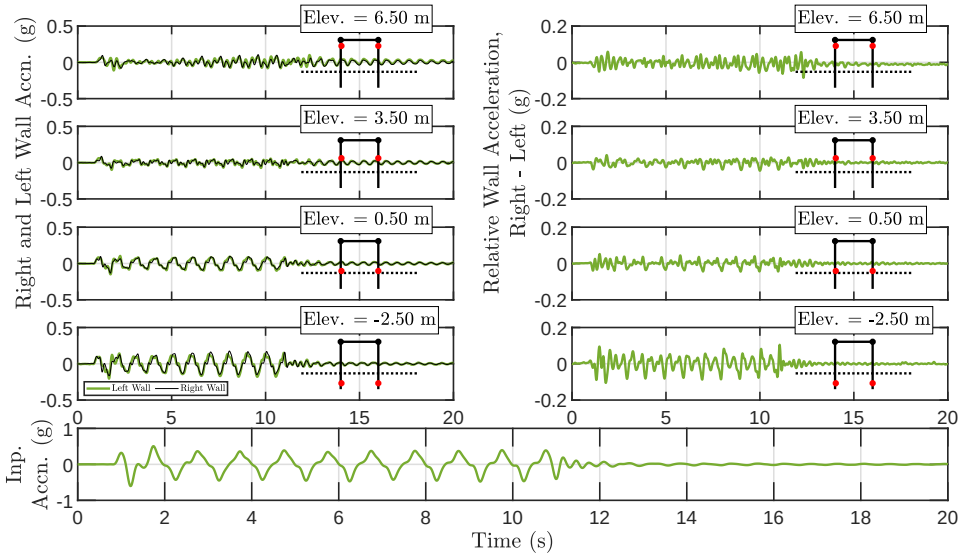
The co-seismic pore pressures and accelerations have hinted at a possible deformation mode for the dual row wall system. Figure 5 presents the results from the series of horizontal LVDTs fixed to an external gantry and spring loaded against the left and right walls. Aversa et al. (2015) describe how the use of LVDTs in this configuration will measure both the model wall movements and effect of the laminae movement, and offer a correction based on assuming symmetric wall displacements. As this assumption may not hold for the present experiments, this adjustment is not made and the LVDTs are only zeroed following swing up

and prior to any shaking. That there is a potential error from global soil translation, which would apply an equal positive and negative error to opposite walls at a given height, should be borne in mind.

Figure 5a shows both the time history of the six LVDTs recording the co-seismic displacements of the left and right wall and the spatial distribution of these same measurements as they progress throughout the shaking. In agreement with the wall accelerations, the left and right wall are confirmed to displace by



(a) Soil accelerations from piezoelectric accelerometers showing de-amplification of accelerations as they propagate upwards through the free field and infill soil



(b) Absolute and relative wall accelerations from MEMs accelerometers revealing cyclic variation of relative acceleration between walls that are broadly accelerated in phase

Figure 4: Time histories of wall and soil accelerations recorded in test WF849

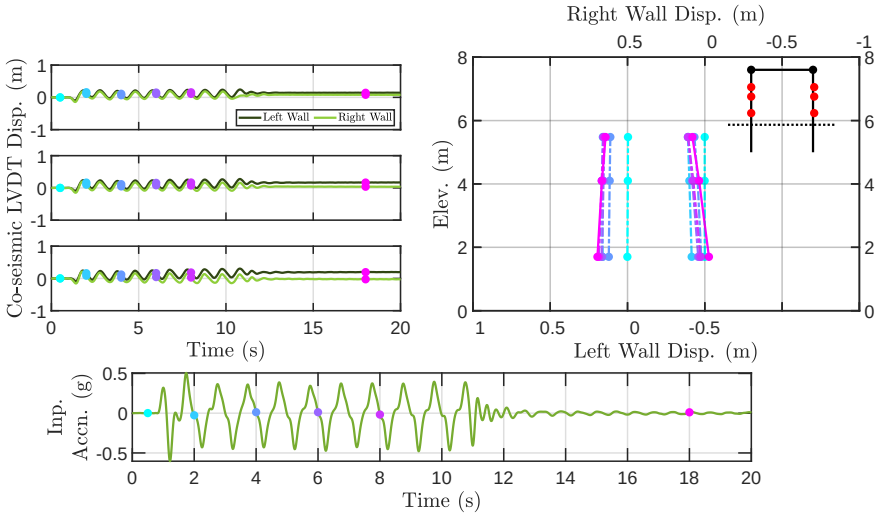
different amounts but in phase and at the driving frequency of the base shaking. Further, fig. 5a confirms the walls open up about the tie rod and that there is a gradual co-seismic accumulation of deformations rather than an instantaneous collapse under the strong cyclic shaking applied. Post shaking no further displacements were observed.

The interdependence between the relative wall displacements and surrounding excess pore pressures is highlighted in fig. 5b. The time history of relative wall displacement confirms that in a given half cycle of acceleration there is a full cycle of relative wall displacement superposed onto the gradual monotonic outward splaying of both walls. As both walls are displaced in one direction, the leading wall moves further into the externally liquefying soil than the lagging wall into the un-liquefied infill. This leads to a drop in excess pore pressure outside the wall due to the tendency for shear dilation and within the wall from the volumetric expansion, rapidly restraining the leading wall and decreasing the relative displacement. As the applied acceleration is reversed the roles of leading and lagging wall will be reversed. The proposed mechanism is consistent with cycling of the external pore pressures, individual wall accelerations and displacements at the driving frequency and also with the relative accelerations, displacements and suctions within the saturated infill at double the driving frequency.

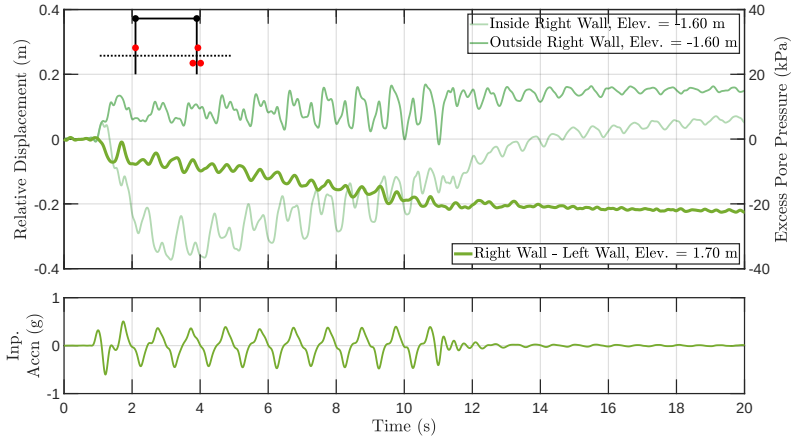
As a result of the excess pore pressure generation, the soil stresses and resulting structural loading will be affected. Figure 6 shows select time histories from the tactile pressure sensors, wall strain gauges and load cells in the tie rods. The total dynamic horizontal stresses in fig. 6 - which in the saturated soil represents the sum of the effective stresses, excess and potentially hydrodyanmic pore pressures - are seen to broadly increase outside the right wall and within the dry infill but decrease within the saturated infill. The horizontal earth pressure coefficient mobilized will tend to unity in fully liquefied soil, which may represent an increase from initially active conditions or decrease from an initially passive state. However, co-seismic cycling of the excess pore pressure, partial mobilization of the passive resistance statically and an increase of soil strength mobilization as the wall displaces can justify the net increase in horizontal total stress observed. The outward wall displacement can also ~~rationalize~~ the reduction in horizontal stresses within the dry infill. The larger and rapid co-seismic reduction and subsequent increase of the total horizontal stress within the saturated infill is consistent with the negative excess pore pressures measured in this region.

The effect of these varying soil stresses on the dual row wall system is captured in fig. 6b. A transition from largely outward to inward bending towards the infill is seen for both walls, simultaneous with a reduction of the tensile force in the connecting tie rod. As with the displacements, the left and right wall exhibit flexure in the same direction and by comporable amounts. The trend of increased external horizontal stress and decreased internal stress measured around the right wall result in an overall decrease of the wall bending that is maintained even as the soil reconsolidates.

Further mechanical insight can be gained from the envelopes and instantaneous distributions of the wall bending and corresponding soil stresses (fig. 7). Madabhushi and Haigh (2021) discussed the predominantly outward bending of stiff dual row walls in dry sand whilst relatively flexible systems exhibited a characterstic S shaped flexure that correpsonds to inward bending towards the wall toe and outward bending with an equilibrating tensile force at the wall head. Accordingly, fig. 7a shows that pre-shaking the wall is relatively stiff in comparison to the saturated soil and features only outward bending. The co-seismic rise and fall of the external and internal stresses result in the inward bending of the lower portion of the wall. As the shaking progresses, fig. 7b reveals that the external soil stresses have further increased whilst a redistribution



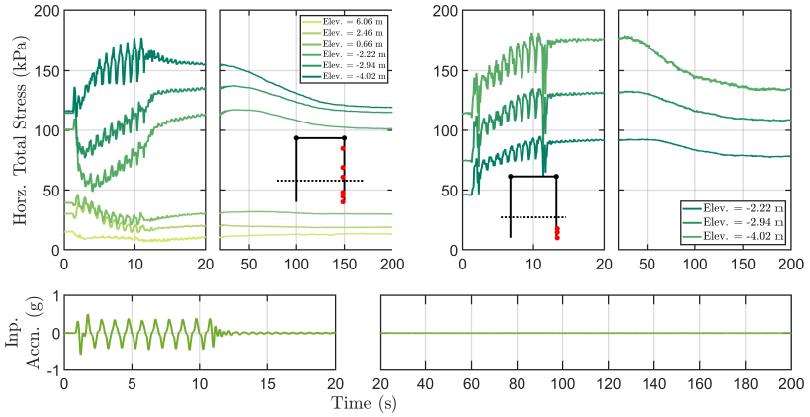
(a) Time histories and select spatial distribution of LVDT measurements highlighting the gradual progression of the outward wall deformations



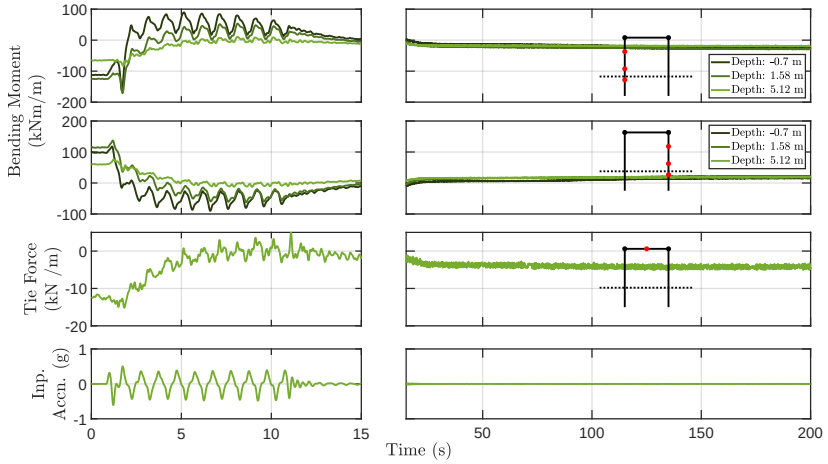
(b) Time histories of relative wall displacement and excess pore pressures around the right wall demonstrating the gradual monotonic progression of the outward splaying mechanism underlying the cycling at double the driving frequency

Figure 5: Displacement measurements from the LVDTs in test WF849

of the internal pressures leads to minimal horizontal stresses within the dry infill. The net result is broadly inward bending of both walls during the shaking with the external and internal saturated soil equilibrating the walls to the extent that there is minimal bending near the wall heads with almost no tie force required. Post-shaking the bending moments remain greatly diminished despite the recovery of the saturated infill stresses. Overall, as a result of the shaking the wall flexure and tie forces are both reduced and from a practical perspective the dynamic demands on the structural componenets may not be critical for design. The relaxation of elastic strain energy stored in the walls and tie rod should be interpretted as a consequence of the wall displacement due to the dynamic soil loading and resistance, rather than the driver for the splaying mode and toe kick out.



(a) Measurements from tactile pressure sensing sheets broadly showing a co-seismic decrease and increase of horizontal total stress within and outside the wall respectively

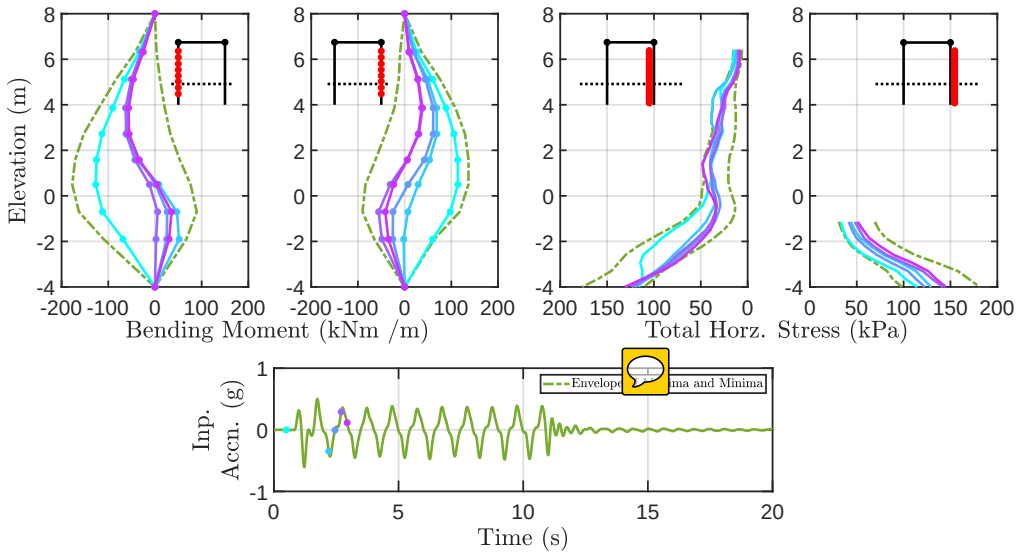


(b) Select strain gauge and load cell measurements showing an overall reversal of bending moment towards the infill and a reduction of tension in the connecting tie rod

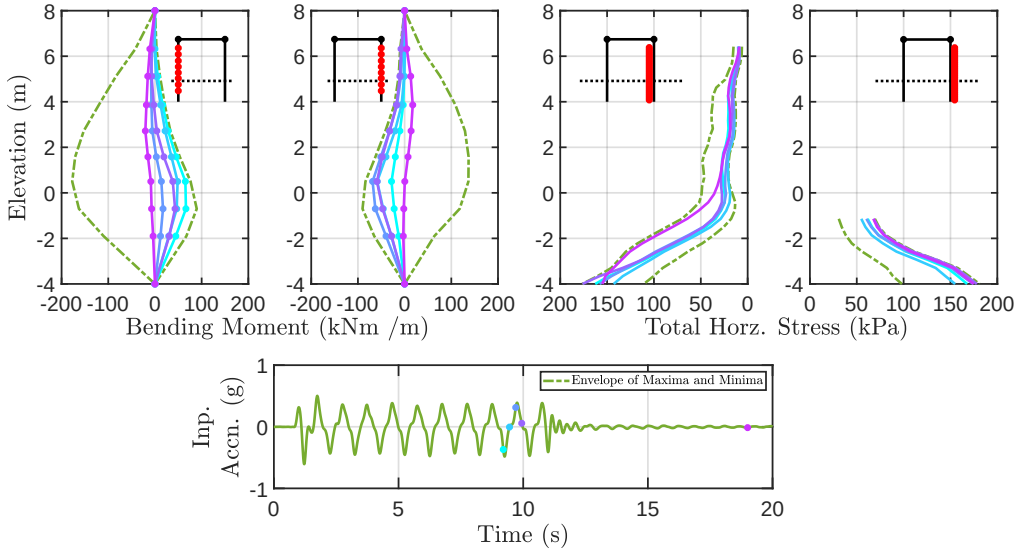
Figure 6: Time histories of horizontal soil stresses, bending moments and tie force in test WF849

3.4 Overall Mechanics

Whilst it is intuitive that a dual row wall system founded in liquefiable soil can deform through outward displacement of the wall toes, the centrifuge experiment reveals a more subtle ratcheting mechanism in which the deformations are cyclically accumulated. Figure 8 presents a combination of the centrifuge measurements to summarize the response of the dual row wall system as the soil liquefies. For the time instants chosen the



(a) Distributions pre-shaking and during early cycling showing predominantly outward bending of the wall and corresponding total horizontal stresses



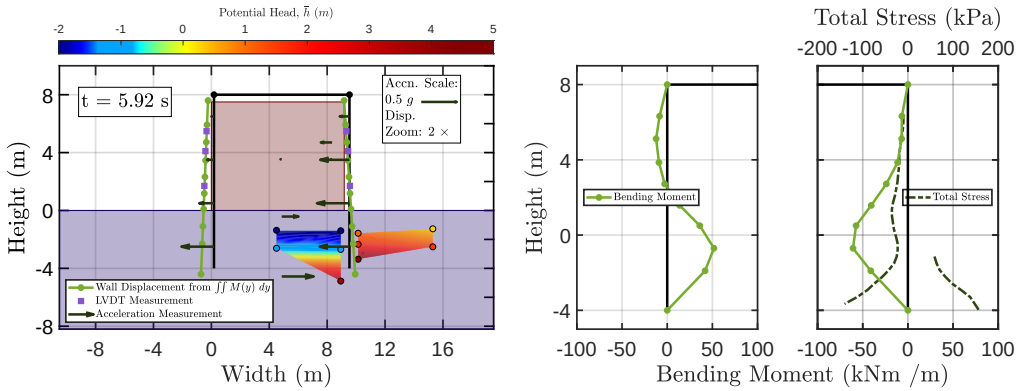
(b) Distributions during a later cycle and post-shaking highlighting the transition to inward bending and corresponding total horizontal stresses

Figure 7: Envelopes and instantaneous distributions of measured bending moments and horizontal total stresses in test WF849

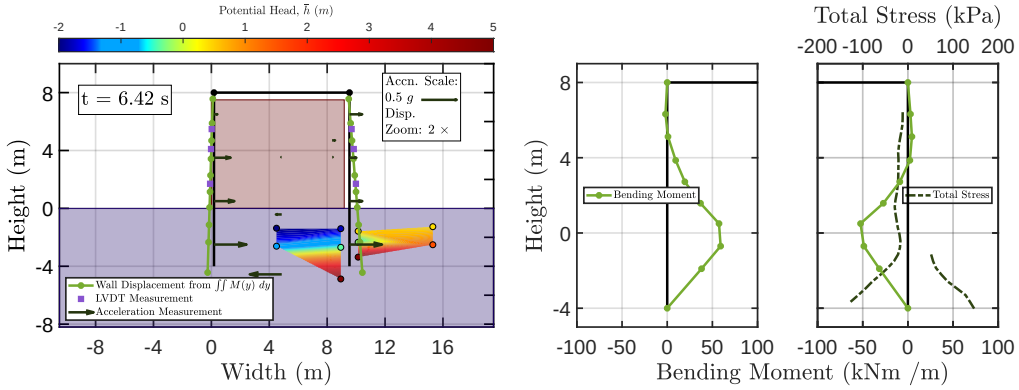
bending moment distributions were double integrated and combined with two LVDT measuremets for each wall to estimate the lateral wall ~~displcaement~~ accounting for each walls flexure, rotation and translation. The third LVDT measurement is plotted to give an indication of consistency. Acceleration vectors from measurements on the wall and in the soil are also shown. The instantaneous distributions of potential head are calculated from the pore pressure data with the datum at the ground surface, i.e. a value of zero indicates hydrostatic conditions. The pore pressures from the transducer affixed to the left wall increased by 4 kPa across the shaking ~~that indicates~~ ~~a~~ settlement of 0.41 m. To provide approximate estimates of vertical wall settlements as shown in fig. 8, the co-seismic rate of settlement was assumed to be constant. Finally, the instantaneous distributions of bending moment and total horizontal stresses measured around the right wall are also plotted.

The overall response across a typical cycle of the sinusoidal loading is shown in figs. 8a to 8c, with figs. 8a to 8b and figs. 8b to 8c spanning half cycles of rightward and leftward acceleration respectively. As previously described, the walls globally cycle in phase but by different amounts as the acceleration direction is reversed. This leads to an opening up of the dual row system about the tie rod as the rotation accrued in one half cycle is not completey reversed in the next. The outward rotation of the walls is driven by the infill soil movement and horizontal stresses, with minimal wall flexure due to the external soil being softened by the positive pore pressures. Crucially however, in each half cycle the wall movement is arrested by both the shear dilation and strength regain of the external soil and increased relative suction between the walls, as captured in fig. 8b. Referring back to fig. 5b the average outward ratcheting of the two walls appears to progress fairly constantly across the loading cycles, despite the fluctuating rates of pore pressure generation and earth pressure changes in the same period. This suggests the soil and structure system is quite stable with broadly compensating changes to the resisting forces developed in response to a change in the driving forces, thus preventing a 'runaway' failure or catastrophic collapse of the dual row system.

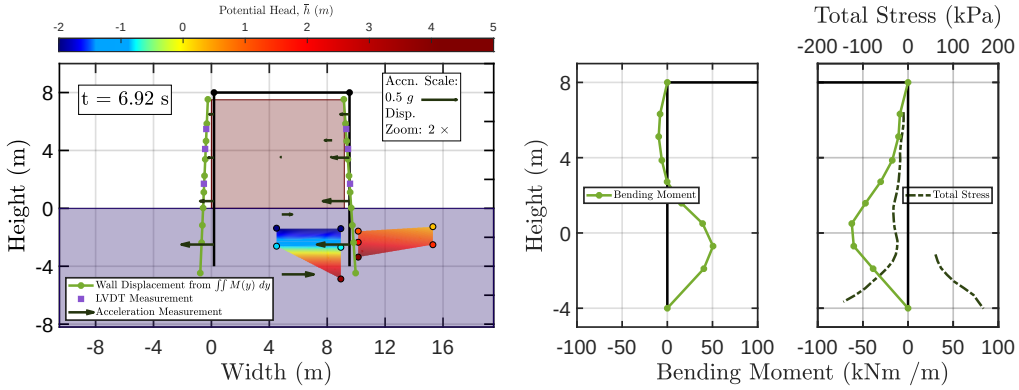
The estimate of the co-seismic vertical settlements shown in fig. 8 are ~~compartively~~ smaller than the horizonal displacement of the wall toes. Experimentally, the limited vertical extent of saturated and loose soil below the dual row system but also the prolonged strong shaking over 10 s should be borne in mind. Overall, the true vertical settlement of a dual row wall system founded in liquefiable soil in the field will depend on the underlying stratigraphy and ~~characterstics~~ of the earthquake it experiences. In the context of their role as a coastal defence, and particularly their resilience to combined earthquake and Tsunami events, the impact of this potential settlement on their post seismic lateral capacity requires further study.



(a) Instant leading to rightward displacement of the right wall into the externally softened soil, driven by infill soil movement and horizontal stresses



(b) Instant of arrested right wall movement due to shear dilation outside the right wall and increased relative suction between the dual row walls



(c) Reversal of accelerations and partial reversal of wall displacements showing some permanent rotation of the right wall has accrued in this cycle

Figure 8: Overall response of the dual row system during a typical cycle of induced liquefaction, constructued using combined measurements of the wall bending, displacement, soil and wall accelerations, horizontal soil stresses and pore pressures

3.5 Conclusions

The centrifuge test has been used to study the complex and coupled dynamic response of the soil and structural elements forming the dual row wall system. A variety of different instrumentation techniques - ranging from measurements of the wall bending and displacements to the pore pressures in the saturated soil and horizontal earth pressures acting on a wall - are considered in turn and in combination to understand the resilience of the system and elucidate the overall mechanical response. In particular, focusing on the frequency of the co-seismic records resutling from a simple single frequency base motion afforded a more direct interpretation of the system mechanics. In contrast to previous studies on dual row retaining walls in dry sand where increased dynamic structural loads and minimal permanent displacements were induced (Madabhushi and Haigh, 2020, 2021), founding the systems in liquefiable soils broadly results in diminished structural demands on the walls and tie rod as permanent displacements are developed. Notably however these displacements were accrued progressively and the system was resilient to a catastrophic collapse under the applied cyclic shaking.

A nuanced understanding of the liquefaction phenomena, including shear dilation outside the walls and the co-seismic migration of pore fluid towards the saturated infill experiencing relative suctions, is required to justify the observed response and resiliency. The cyclic regain of the external soil strength and stiffness, in addition to the inceased liquefaction resistance from increased vertical and horizontal effective stresses from the dry infill and wall equilibrium, are important considerations. A ratcheting mechanism for the wall deformations was identifed based on the experimental measurements. In a given half cycle of acceleration the leading wall displaces away from the infill and lagging wall and this change is not completley reversed in the subsequent half cycle. The proposed mechanism is consistent with cycling of the external pore pressures and displacements at the driving frequency and also with the relative displacement between the two walls and suctions within the saturated infill at double the driving frequency.

Whilst the simple, symmetric base motion applied was important to allow interpretation of the mechanical response, the dependence of the system's seismic ~~resiliency~~ on the shaking characterstics requires further study. In particular, the rate of progress of the ratcheting mechanism may be increased if the seismic excitation features asymmetric pulses that do not result in the partial recovery of each wall rotation in alternating half cycles. Nevertheless, the experimental results and proposed mechanism challenge conventionally conservative design strategies, in particular that the sheet pile walls must extend completely below a liquefiable layer to prevent catastrophic collapse.

References

Arulanandan, K., Manzari, M., Zeng, X., Fagan, M., Scott, R. F. and Tan, T. S. (1995). Significance of the VELACS project to the solution of boundary value problems in geotechnical engineering, *3rd International conference, Recent advances in geotechnical earthquake engineering and soil dynamics*, University of Missouri, Rolla, St Louis, pp. 825–832.

Aversa, S., de Sanctis, L., Maiorano, R. M. S., Tricarico, M., Viggiani, G. M. B., Conti, R. and Madabhushi, S. P. G. (2015). Centrifuge modelling of retaining walls embedded in saturated sand under seismic actions, *Geotechnical, Geological and Earthquake Engineering* **35**: 543–562.

Azeiteiro, R. J. N., Coelho, P. A. L. F., Taborda, D. M. G. and Grazina, J. C. D. (2017). Critical State – Based Interpretation of the Monotonic Behavior of Hostun Sand, *Journal of Geotechnical and Geoenvironmental Engineering* **143**(5): 1–14.

Brennan, A. J., Madabhushi, S. P. G. and Houghton, N. (2006). Comparing laminar and equivalent shear beam (ESB) containers for dynamic centrifuge modelling, *in* C. W. W. Ng, L. M. Zhang and Y. H. Wang (eds), *Physical modelling in geotechnics : 6th ICPMG '06*, Vol. 1-2 of *Balkema-proceedings and monographs in engineering, water and earth sciences*, Taylor & Francis, United Kingdom, pp. 171–176.

Casagrande, A. (1936). Characteristics of cohesionless soils affecting the stability of slopes and earth fills, *Journal of Boston Society of Civil Engineering* **23**(1): 257–276.

Castro, G. (1969). *Liquefaction of sands*, PhD thesis, Harvard University, Cambridge, Massachusetts.

Castro, G. and Poulos, S. J. (1977). Factors affecting liquefaction and cyclic mobility, *Journal of Geotechnical and Geoenvironmental Engineering* **103**(6): 501–506.

Chen, C.-H. and Hwang, G. (2000). Preliminary analysis for quay wall movement in Taichung Harbour during the September 21, 1999, Chi-Chi earthquake, *Earthquake Engineering and Engineering Seismology* **2**(1): 43–54.

Choudhury, D. and Nimbalkar, S. S. (2006). Pseudo-dynamic approach of seismic active earth pressure behind retaining wall, *Geotechnical and Geological Engineering* **24**(5): 1103–1113.

Cummins (n.d.). Giken, Silent Piler drives critical tsunami defence work.

Elgamal, A. W., Dobry, R., Parra, E. and Yang, Z.-h. (1998). Soil Dilation and Shear Deformations During Liquefaction, *Fourth International Conference on Case Histories in Geotechnical Engineering* pp. 1238–1259.

Haigh, S. K., Eadington, J. and Madabhushi, S. P. G. (2012). Permeability and stiffness of sands at very low effective stresses, *Geotechnique* **62**(1): 69–75.

Inatomi, T., Zen, K., Toyama, S., Uwabe, T., Iai, S., Sugano, T., Terauchi, K. and Yokota, H. (1997). Damage to Port and Port-related Facilities by the 1995 Hyogoken-nanbu Earthquake, *Technical report*, Japan: The Portand Harbour Research Institute.

Ishihara, K. (1985). Stability of natural deposits during earthquakes, *Proc. 11th international conference on soil mechanics and foundation engineering*, Balkema, San Francisco, pp. 321–376.

Kutter, B. L., Manzari, M. T. and Zeghal, M. (2020). *Model Tests and Numerical Simulations of Liquefaction and Lateral Spreading*.

Kutter, B. L. and Wilson, D. W. (1999). De-liquefaction shock waves, *Proceedings of the Seventh U.S.-Japan Workshop on Earthquake Resistant Design of Lifeline Facilities and Countermeasures Against Soil Liquefaction*, pp. 295–309.

Lakeland, D. L., Rechenmacher, A. and Ghanem, R. (2014). Towards a complete model of soil liquefaction: the importance of fluid flow and grain motion, *Proceedings of the Royal Society A: Mathematical, Physical and Engineering Sciences* **470**(2165): 20130453.

Luong, M. P. and Sidaner, J. F. (1981). Undrained behaviour of cohesionless soils under cyclic and transient loading, *Proceedings: First International Conference on Recent Advances in Geotechnical Earthquake Engineering and Soil Dynamics*, University of Missouri–Rolla, pp. 215–220.

Madabhushi, S. P. G. and Haigh, S. K. (2012). How Well Do We Understand Earthquake Induced Liquefaction?, *Indian Geotechnical Journal* **42**(3): 150–160.

Madabhushi, S. P. G., Houghton, N. E. and Haigh, S. K. (2006). A new automatic sand pourer for model preparation at University of Cambridge, *Proceedings of the Sixth International Conference on Physical Modelling in Geotechnics*, Taylor & Francis, Hong Kong, pp. 217–222.

Madabhushi, S. P. G. and Zeng, X. (2007). Simulating seismic response of cantilever retaining walls, *Journal of Geotechnical and Geoenvironmental Engineering* **133**(5): 539–549.

Madabhushi, S. S. C. (2018). *Multi-Hazard Modelling of Dual Row Retaining Walls*, Phd thesis, University of Cambridge.

Madabhushi, S. S. C. and Haigh, S. K. (2018a). A Comparison between the Dynamic Behaviour of Flexible Dual Row Walls Founded in Dry and Liquefiable Sands, *1st International Conference on Press-in Engineering*, pp. 265–272.

Madabhushi, S. S. C. and Haigh, S. K. (2018b). Using Tactile Pressure Sensors to Measure Dynamic Earth Pressures around Dual Row Walls, *International Journal of Physical Modelling in Geotechnics* **19**(2): 58–71.

Madabhushi, S. S. C. and Haigh, S. K. (2019). Centrifuge Testing of Dual Row Walls in Dry Sand: the influence of Earthquake sequence and multiple flights, *Soil Dynamics and Earthquake Engineering* **125**.

Madabhushi, S. S. C. and Haigh, S. K. (2020). Dual Row Retaining Walls in Dry Sand: The Influence of Wall Stiffness on the Seismic Response, *Canadian Geotechnical Journal* .

Madabhushi, S. S. C. and Haigh, S. K. (2021). On the Dynamic Response of Flexible Dual Row Retaining Walls in Dry Sand, *Géotechnique* pp. 1–32.

Mononobe, N. and Matsuo, H. (1929). On determination of earth pressure during earthquake, *Proceedings of the World Engineering Congress, Tokyo*, Vol. 9, Kogakkai, Tokyo, Japan, p. 176.

Okabe, S. (1924). General Theory on Earth Pressure and Seismic Stability of Retaining Wall and Dam, *Journal of Japan Society of Civil Engineers* **10**(6): 1277–1323.

Otsushi, K., Fuiwwara, K., Yoshihara, K., Nishibe, K., Kurosawa, T., Toda, K., Okuda, Y. and Kurosaki, K. (2016). Coastal Dyke and Tide Barrier Technologies for Large Earthquakes and Tsunami Runups, *Nippon Steel & Sumitomo Metal Corporation researches and develops solution technol- ogy related to the reinforcement and renovation of coastal protection facilities, such as coastal dykes and tide barriers, as the countermeasure against large earthquake a* (113).

Paikowsky, S. G. and Hajduk, E. L. (1997). Calibration and Use of Grid-Based Tactile Pressure Sensors in Granular Material, *Geotechnical Testing Journal* **20**(2): 218–241.

Roscoe, K. H., Schofield, A. N. and Wroth, C. P. (1958). On the yielding of soil, *Géotechnique* **8**(1): 22–52.

Schofield, A. N. (1980). Cambridge Geotechnical Centrifuge Operations, *Géotechnique* **30**(3): 227–268.

Steedman, R. S. and Zeng, X. (1990). The influence of phase on the calculation of pseudo-static earth pressure on a retaining wall, *Géotechnique* **40**(1): 103–112.

Stewart, D. P., Chen, Y.-R. and Kutter, B. L. (1998). Experience with the Use of Methylcellulose as a Viscous Pore Fluid in Centrifuge Models, *Geotechnical Testing Journal* **21**(4): 365.

Stringer, M. E. and Madabhushi, S. P. G. (2009). Novel computer-controlled saturation of dynamic centrifuge models using high viscosity fluids, *Geotechnical Testing Journal* **32**(6).

Sumer, B. M., Kaya, A. and Hansen, N. E. O. (2002). Impact of liquefaction on coastal structures in the 1999 Kocaeli, Turkey earthquake, *Proceedings of the International Offshore and Polar Engineering Conference* **12**: 504–511.

Zeng, X. and Steedman, R. S. (1993). On the behaviour of quay walls in earthquakes, *Géotechnique* **43**(3): 417–431.